

**Introduction to the simulation of direct
radiative forcing of aerosols and their
effects on East Asian climate using an
interactive AGCM–aerosol coupled
system in CMA, China**

**Hua Zhang Z.-L. Wang Z. Z. Wang Q. X. Liu S. L.
Gong X. Y. Zhang and Co-authors**

**National Climate Center
China Meteorological Administration**

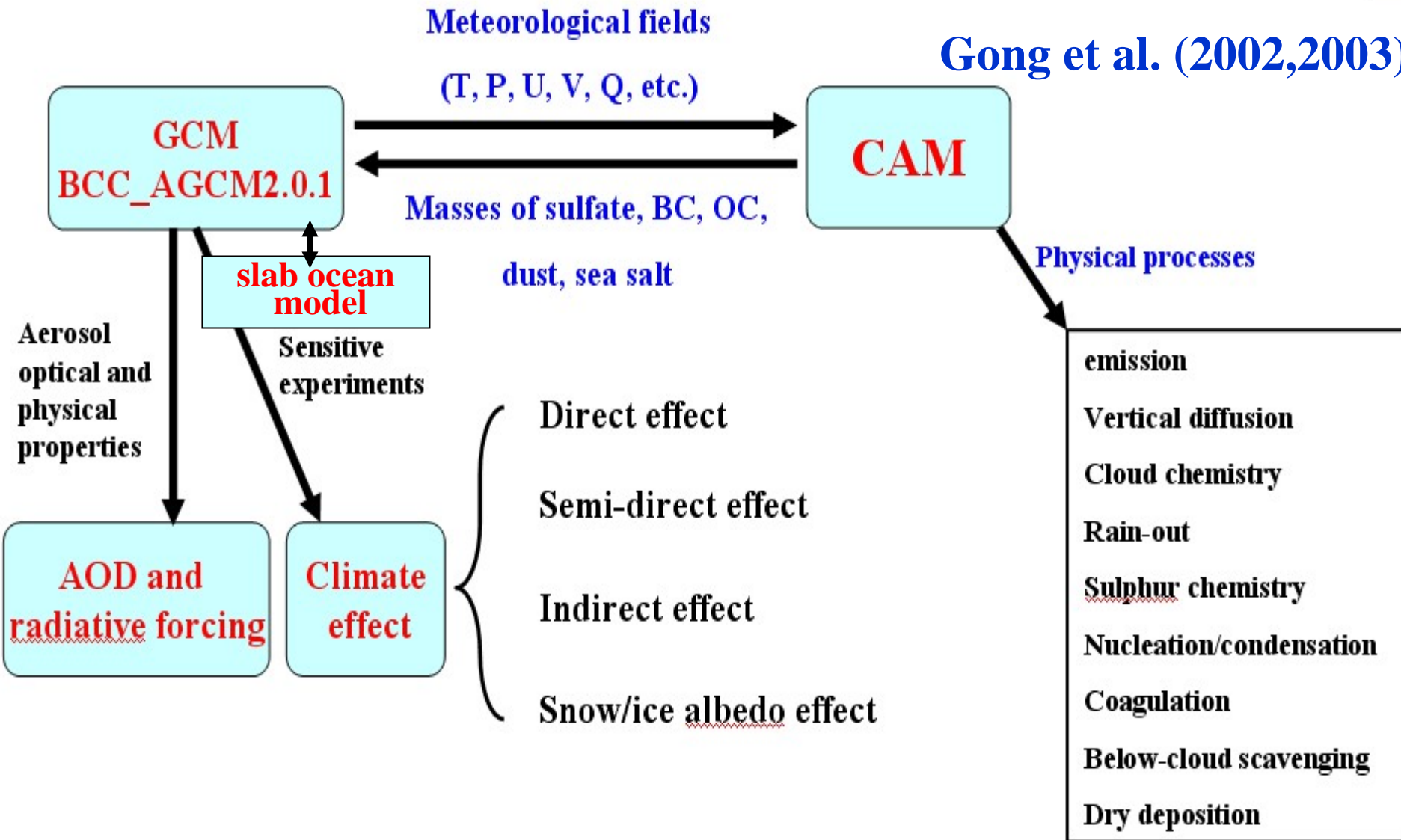
**AeroCom Workshop, Fukugawa, Japan
Oct. 3-6, 2011**

Outline

- **Model description**
- **Simulated aerosol concentrations and optical properties**
- **Simulated direct radiative forcings due to aerosols**
- **Conclusion of the effect of sulfate, BC and OC aerosols on East Asian summer monsoon**
- **Publications**

Our Work

Gong et al. (2002,2003)



Model description

BCC_AGCM2.0.1 was developed by the National Climate Center of the China Meteorological Administration (**NCC/CMA**).

□ **Dynamic core:** Eulerian dynamical core

□ **Horizontal resolution:** T42 (approximating $2.8^\circ \times 2.8^\circ$)

□ **Vertical direction:** hybrid sigma-pressure coordinate system, 26 layers, the top layer: 2.9 hPa.

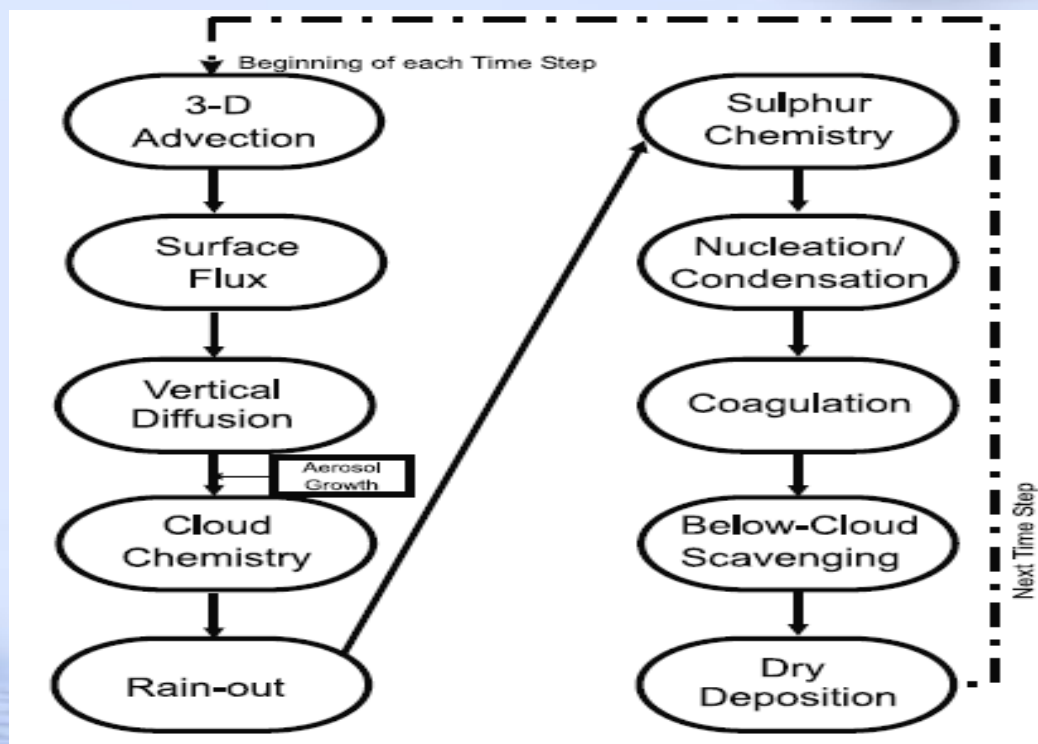
□ **Radiation Scheme:** 19 bands for SW, two-stream δ -Eddington approximation.

□ In this study, BCC_AGCM2.0.1 was coupled with a **slab ocean model**.

Compared to CAM3, a few improvements have been implemented in BCC_AGCM2.0.1. The dynamics in the model differs significantly from the Eulerian spectral formulation of the CAM3, and reference stratified atmospheric temperature and surface pressure were introduced into the governing equations to improve calculation of the pressure gradient force and the gradients of surface pressure and temperature (Wu et al. 2008). The major modifications to the model physics included a new convection scheme (Zhang and Mu 2005), a dry adiabatic adjustment scheme in which potential temperature is conserved (Yan 1987), a modified scheme to calculate sensible heat and moisture fluxes over open ocean that considers the effect of ocean waves on latent and sensible heat fluxes (Wu et al. 2010), and an empirical equation to compute the snow cover fraction (Wu and Wu 2004). The model provides overall improvements to climate simulations in comparison to CAM3, especially for simulating the tropical maxima/sub-tropical minima of precipitation, wind stress, and sensible and latent heat fluxes at the ocean surface (Wu et al. 2010).

Canadian Aerosol Module (CAM)

- ❑ CAM, a **size-segregated multi-component aerosol algorithm**, was developed by Gong et al. (2002; 2003). Five aerosol species were taken into account, including **sulfate, BC, OC, soil dust, and sea salt**.



The flowchart of process splitting in CAM

□ The aerosol size spectrum was divided into **12 bins** between **0.005~20.48** μm . The effective radius of the aerosols was taken as the average value in each bin.

1	2	3	4	5	6	7	8	9	10	11	12
0.005 ~0.01	0.01~ 0.02	0.02~ 0.04	0.04~ 0.08	0.08~ 0.16	0.16~ 0.32	0.32~ 0.64	0.64~ 1.28	1.28~ 2.56	2.56~ 5.12	5.12~ 10.24	10.24~ 20.48

□ The **source emissions of aerosol** were derived primarily from **AeroCom** data, including the surface emission rate of both natural and anthropogenic aerosols: **BC and OC** (Van der Werf et al. 2004; Bond et al. 2004), **SO₂ and sulfate** (Van der Werf et al. 2004; Cofala et al. 2005), and **dimethyl sulfide (DMS)** (Kettle and Andreae [2000] for ocean data; Nightingale [2000] for air-sea transfer). The **sea salt** module was developed by Gong et al. (2002), and the **soil dust** scheme was from Marticorena and Bergametti (1995).

Simulated aerosol concentrations and optical properties

- The aerosol optical properties (**extinction coefficient, single scattering albedo, and asymmetry parameter**) were calculated using Mie scattering theory.
- The **hygroscopic growth** of soluble aerosol particles (sulfate, OC, and sea salt) was also taken into account.
- All types of aerosol are **externally mixed** in the model to calculate the aerosol optical properties and radiative forcings.

The refractive index and densities of dry aerosols

Table 1 The refractive index and densities of dry aerosols

Component	Refractive index ($\lambda = 0.55 \mu\text{m}$)	Density (kg m^{-3})
Sulfate	$1.43 - 1.0 \times 10^{-8} i$	1,769.0
BC	$1.75 - 0.44 i$	1,500.0
OC	$1.53 - 0.0059 i$	1,300.0
Dust	$1.53 - 0.008 i$	2,650.0
Sea salt	$1.5 - 9.7 \times 10^{-9} i$	2,170.0

The radius growth of the three species aerosol particles with RH

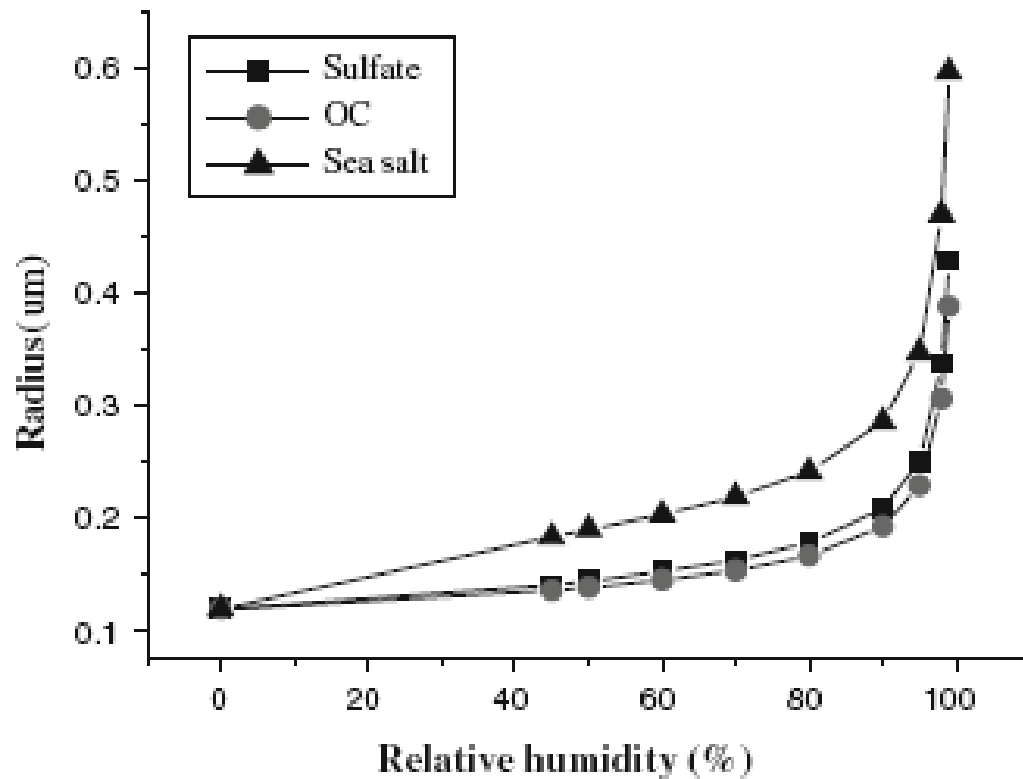
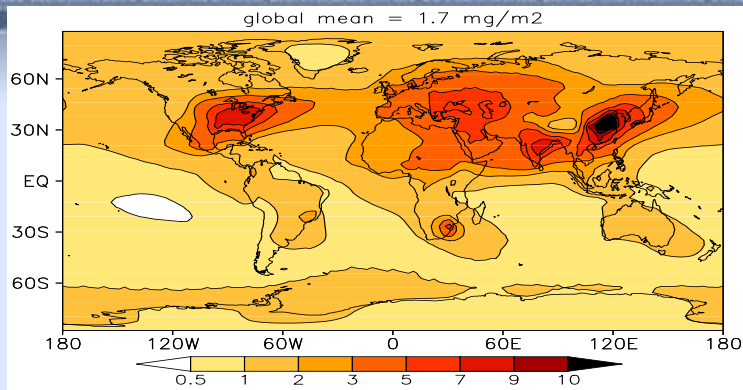
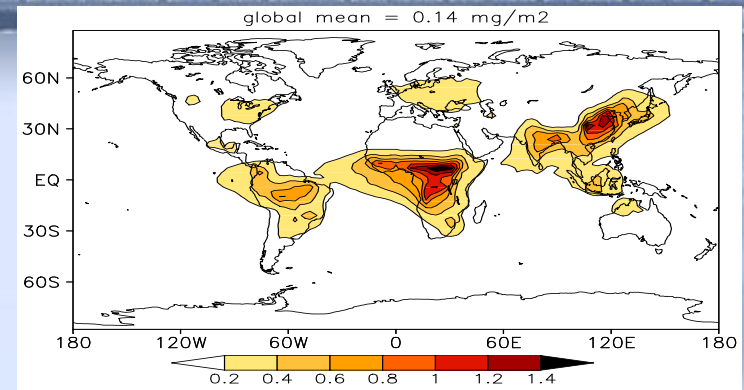


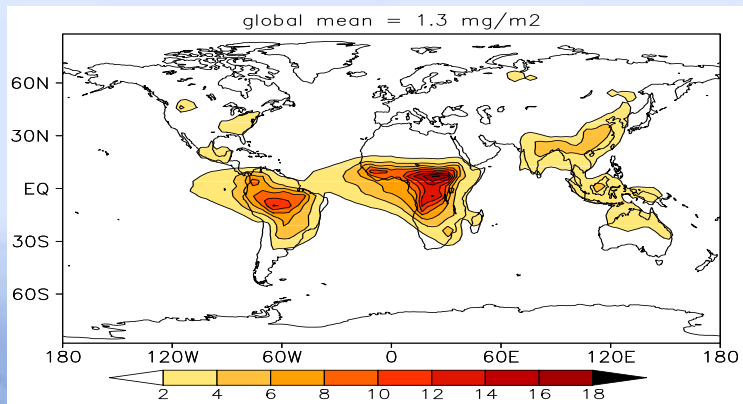
Fig. 1 The radius growth of the three species of hygroscopic aerosol particles with increasing relative humidity



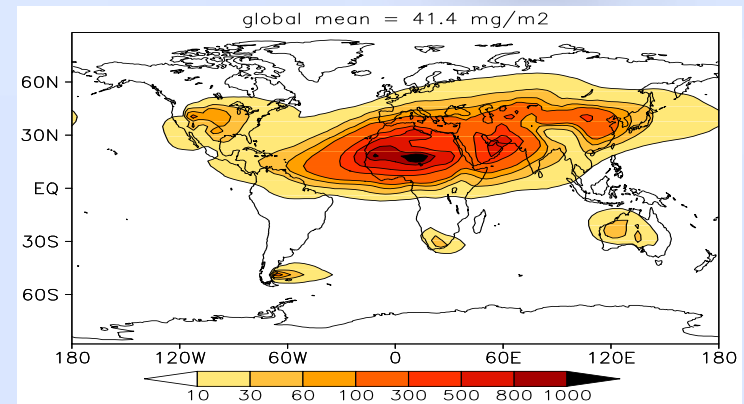
Sulfate



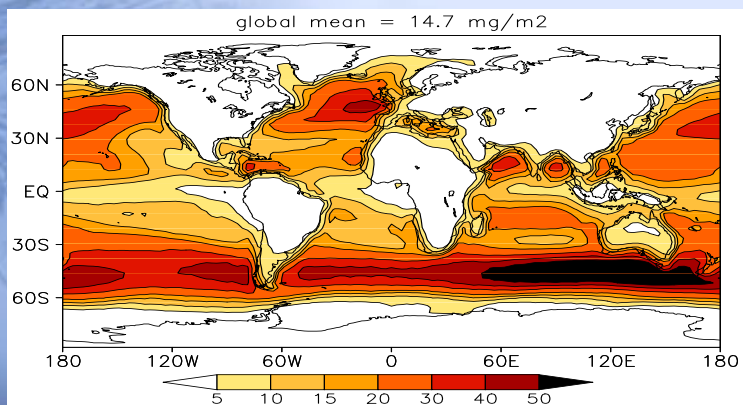
BC



OC



Dust

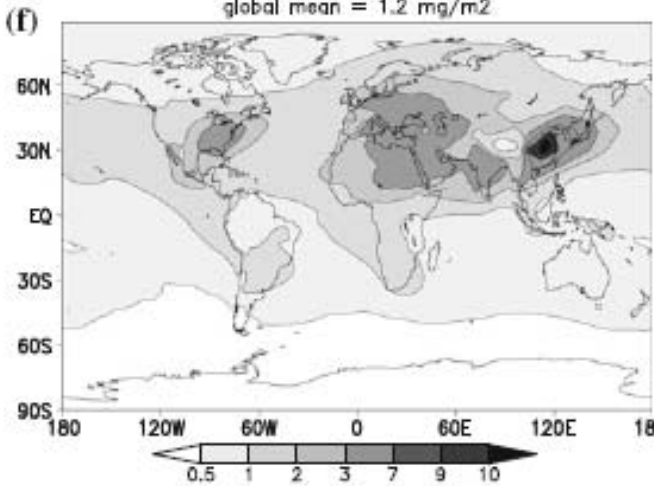


Sea-salt

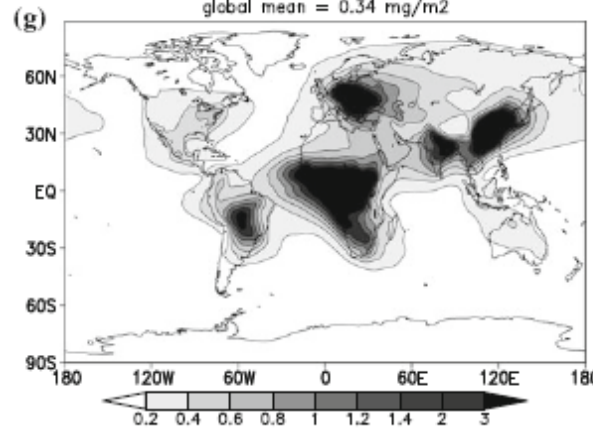
**Global distribution of simulated
aerosol column burdens
(mg m⁻²)**

Global distribution of AEROCOM-MEDIAN (mg m^{-2})

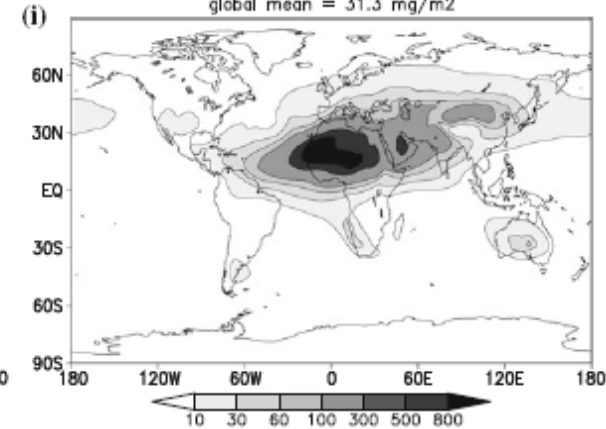
global mean = 1.2 mg/m^2



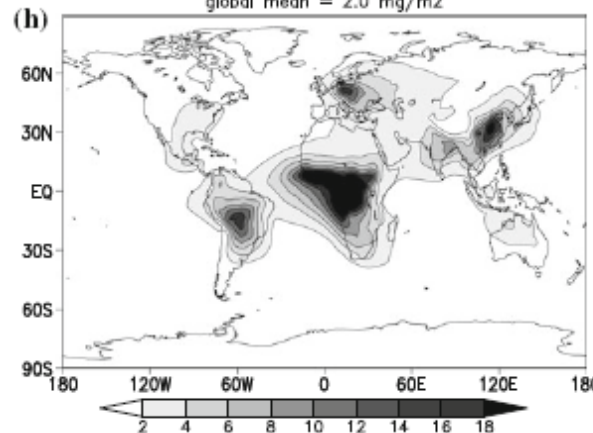
global mean = 0.34 mg/m^2



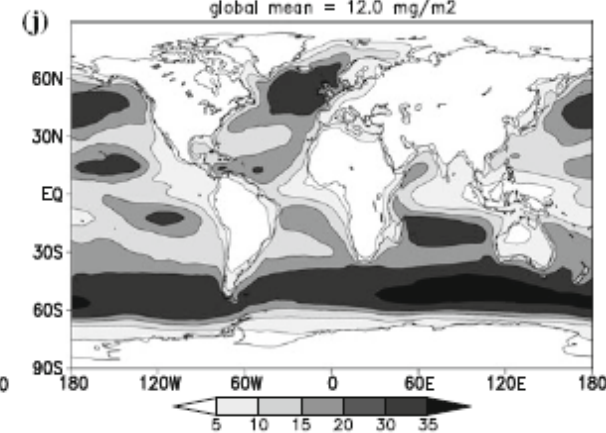
global mean = 31.3 mg/m^2

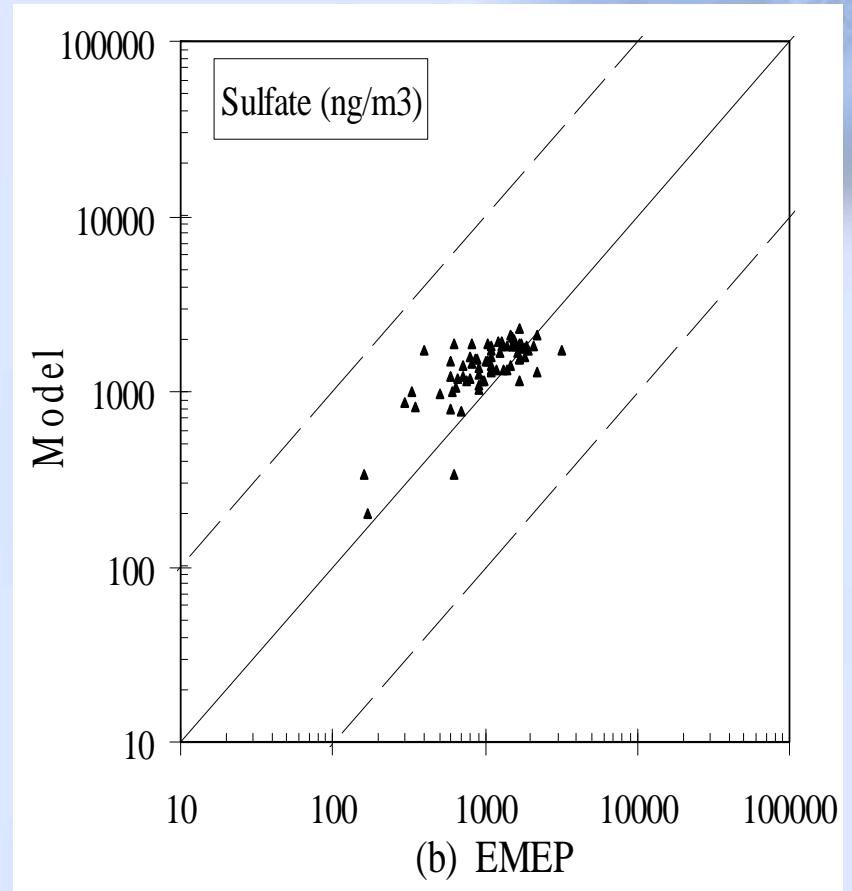
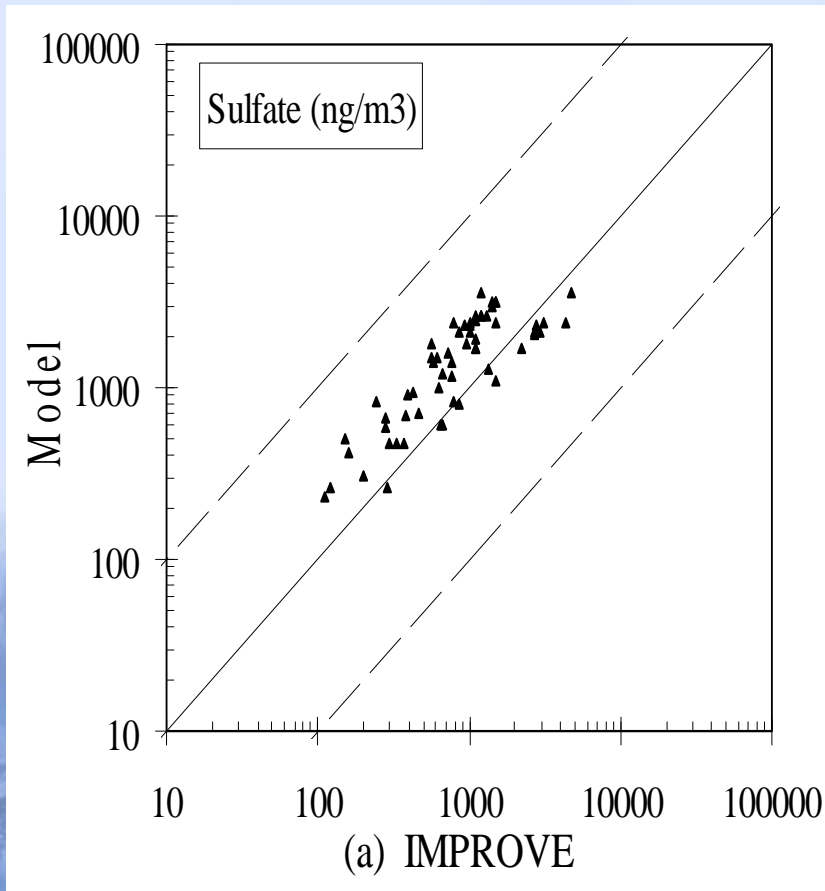


global mean = 2.0 mg/m^2

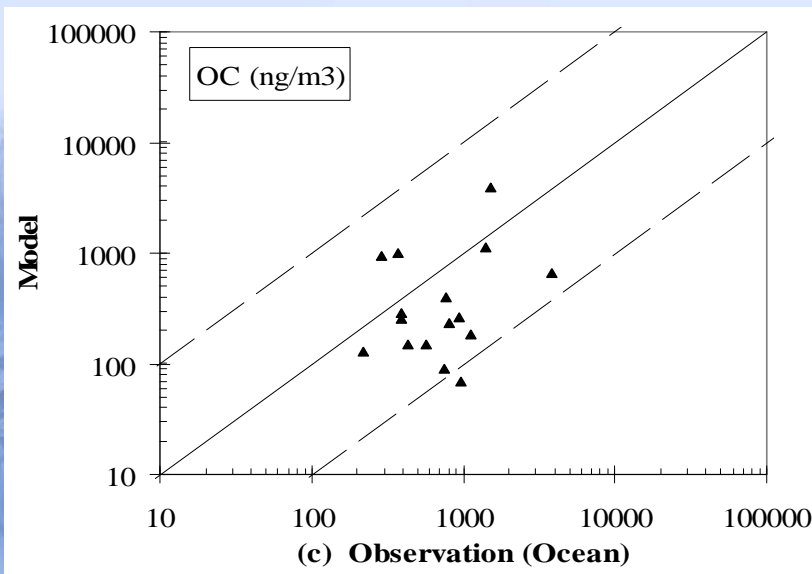
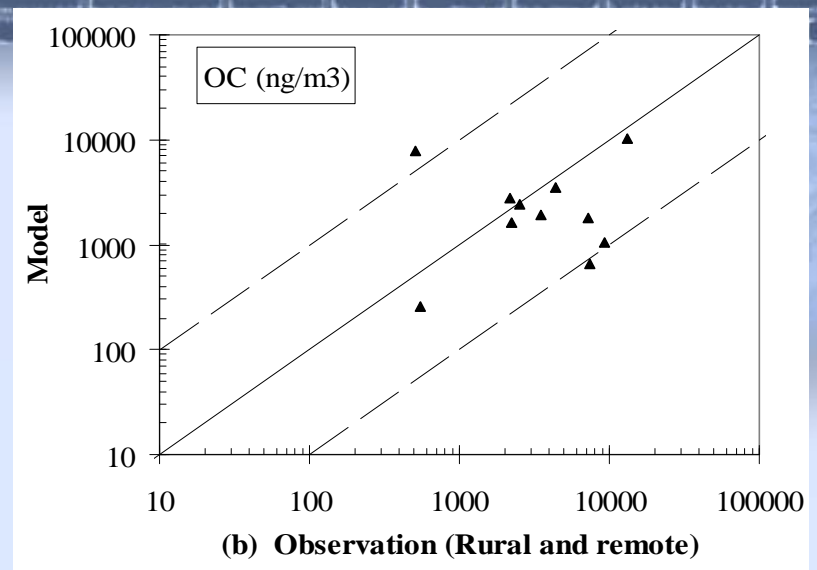
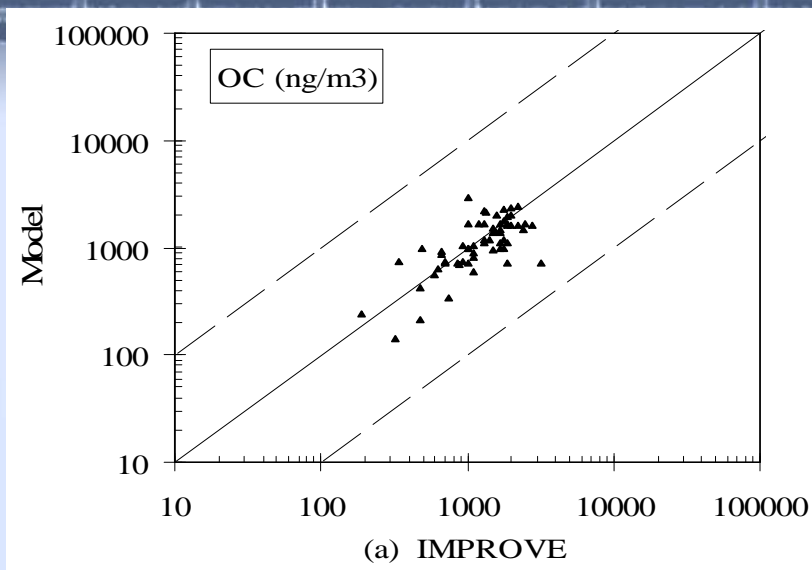


global mean = 12.0 mg/m^2



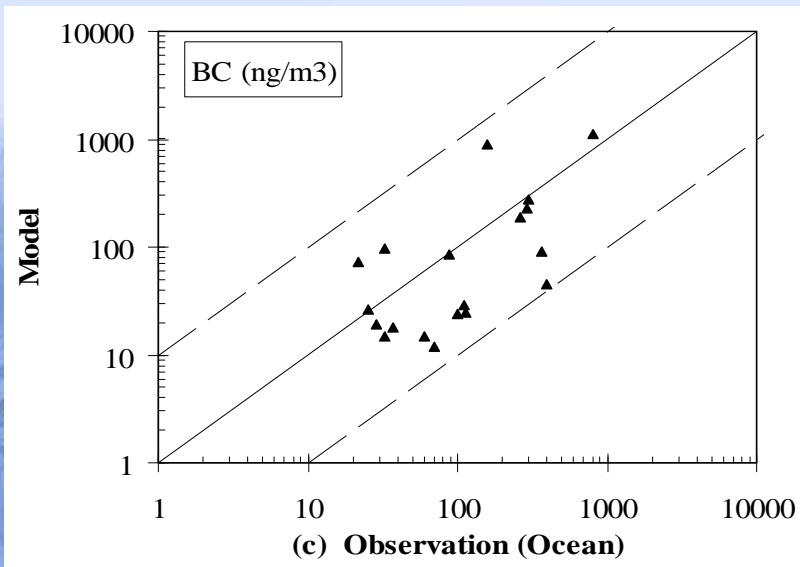
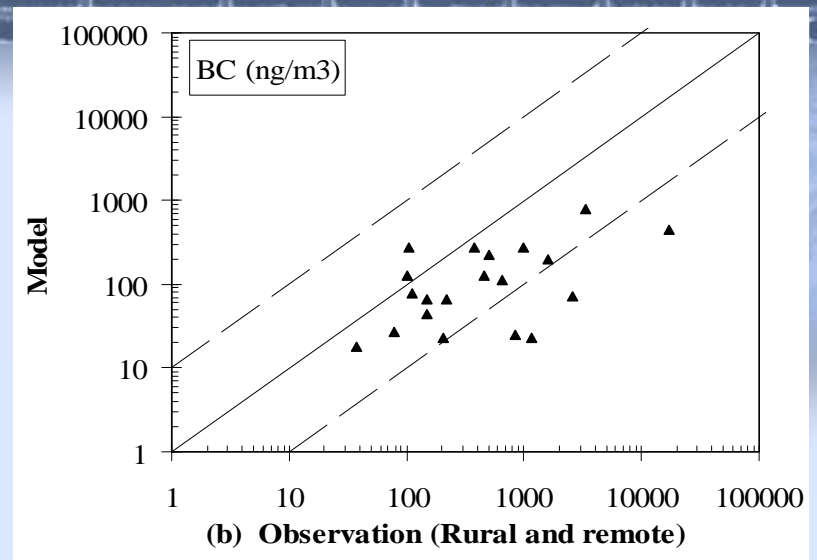
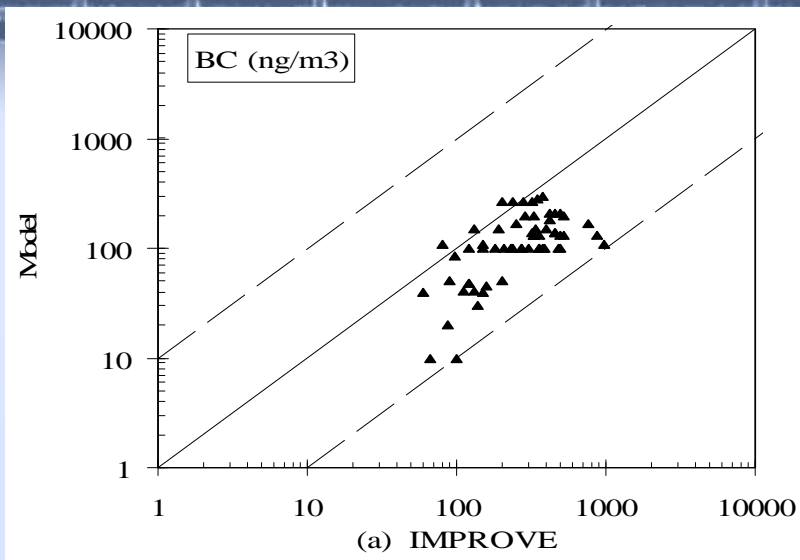


Simulated sulfate concentrations versus observations for (a) IMPROVE sites, (b) EMEP sites. The dashed lines indicate 10:1 and 1:10 ratios.



OC concentrations was underestimated in rural and remote sites and marine sites.

Simulated OC concentrations versus observations for (a) IMPROVE sites, (b) rural and remote sites, and (c) marine sites. The dashed lines indicate 10:1 and 1:10 ratios.

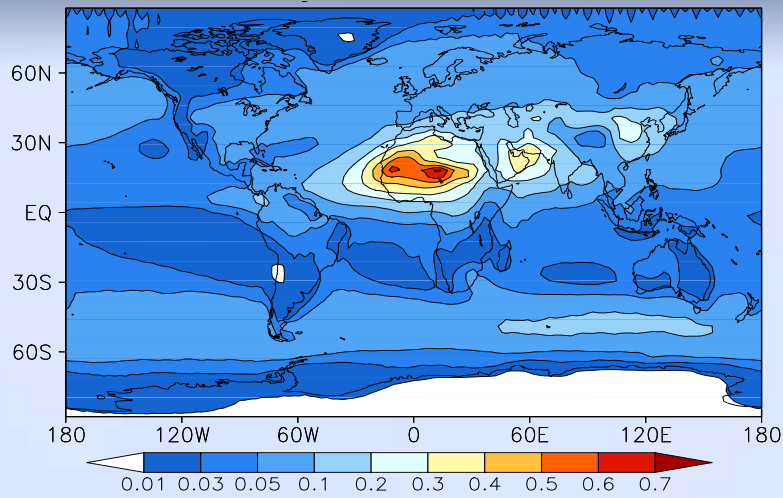


BC concentrations was underestimated as a whole.

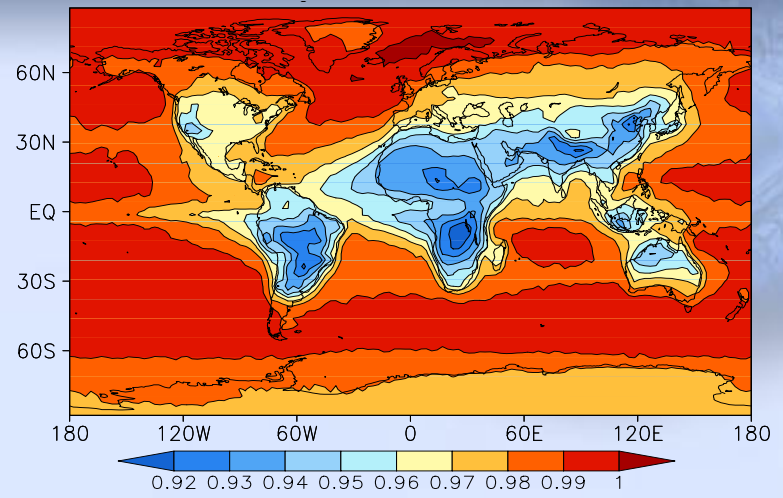
Simulated BC concentrations versus observations for (a) IMPROVE sites, (b) rural and remote sites, and (c) marine sites. The dashed lines indicate 10:1 and 1:10 ratios.

Summary of the global emission and burden of BC

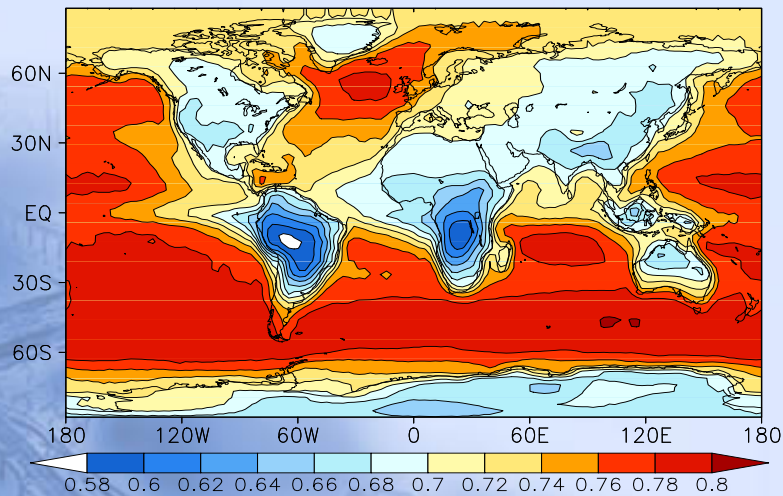
Model	Emission (Tg year ⁻¹)	Burden (Tg)	References
Our study	7.7	0.07	Dentener et al. (2006)
GISS	12.41	0.14	Koch (2001)
MIRAGE	14.0	0.22	Easter et al. (2004)
LMDZT	10.5	0.19	Reddy et al. (2005)
GOCART	13.7	0.27	AEROCOM
PNNL	11.4	0.19	AEROCOM
IPCC-TAR	12.3		Dentener et al. (2006)



(a)



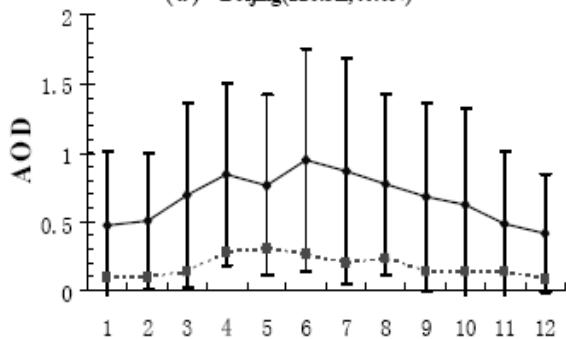
(b)



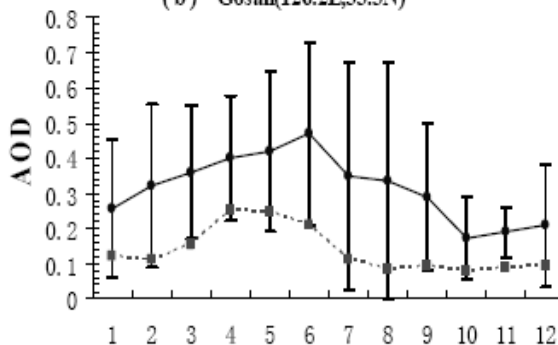
(c)

Global annual mean distributions of simulated (a) total AOD, (b) single scattering albedo and (c) asymmetry parameter at 550 nm

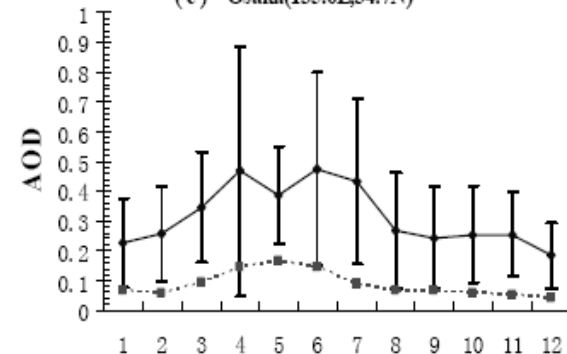
(a) Beijing(116.3E,40.0N)



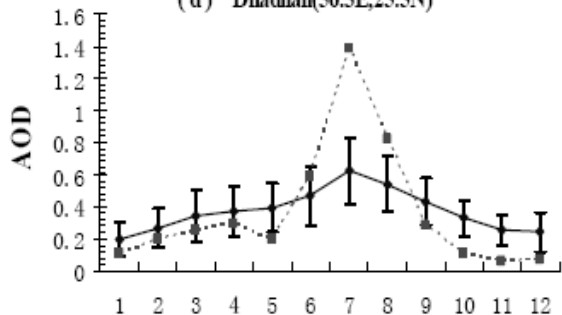
(b) Gosan(126.2E,33.3N)



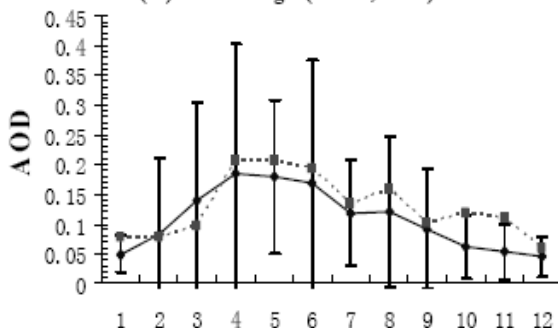
(c) Osaka(135.6E,34.7N)



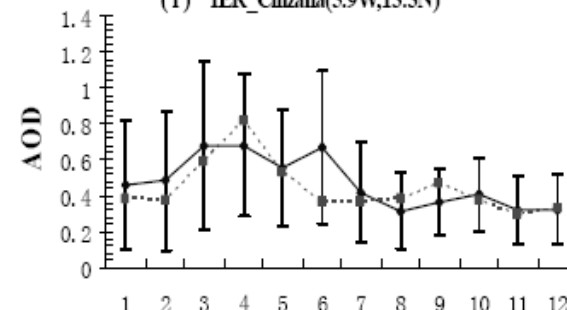
(d) Dhahnah(56.3E,25.5N)



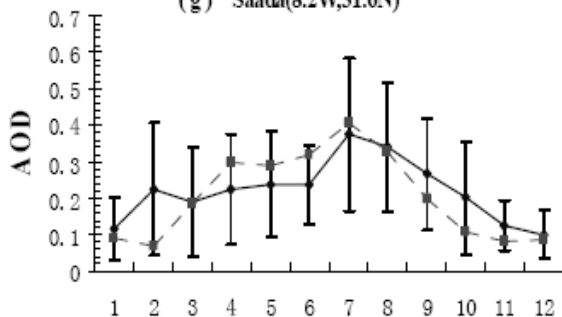
(e) Dalanzadgad(104.4E,43.6N)



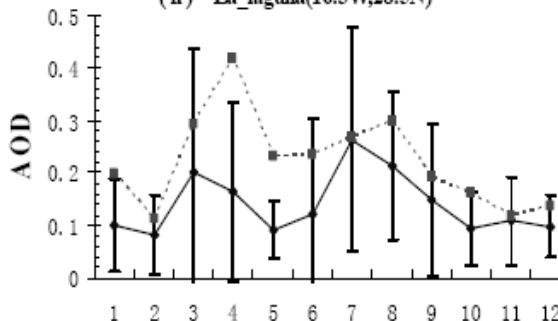
(f) IER_Cinzana(5.9W,13.3N)



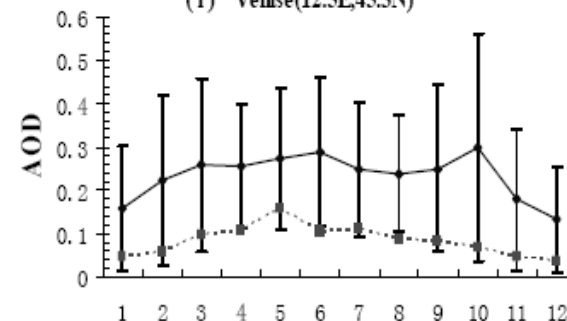
(g) Saada(8.2W,31.6N)



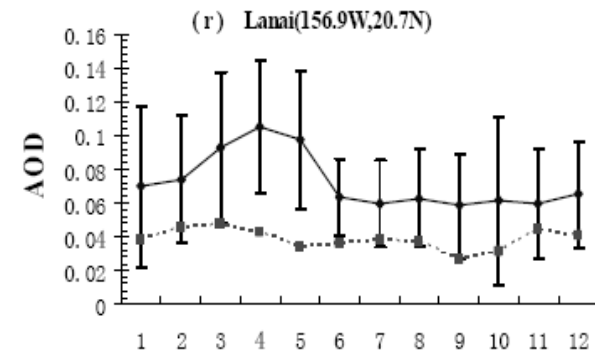
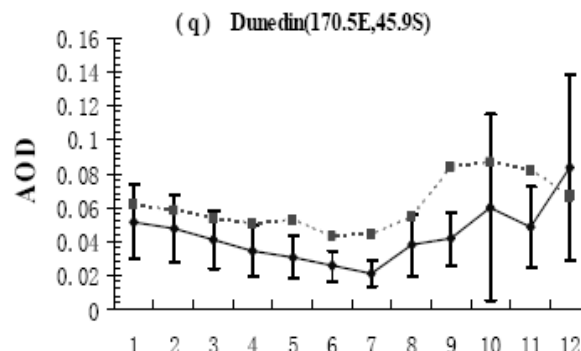
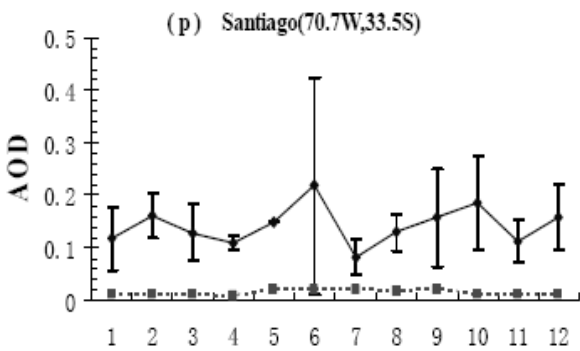
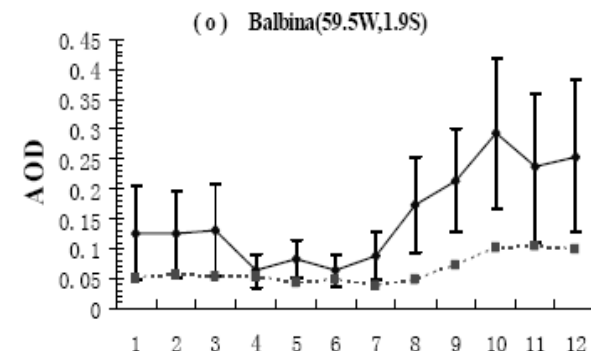
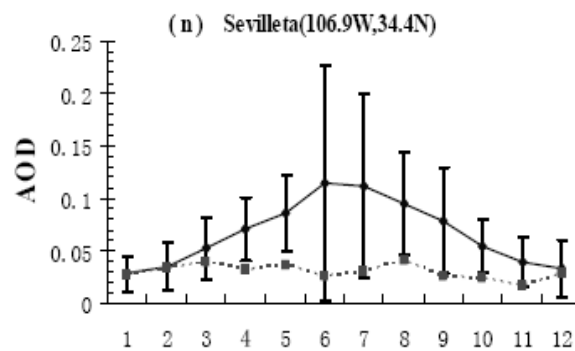
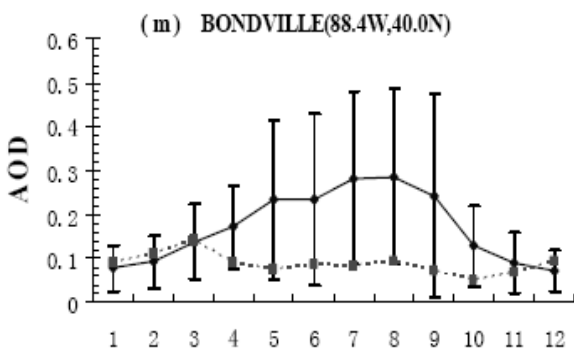
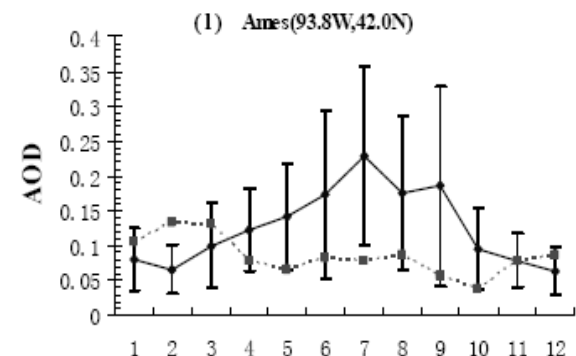
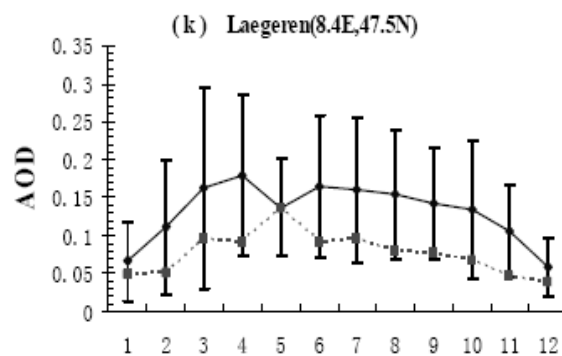
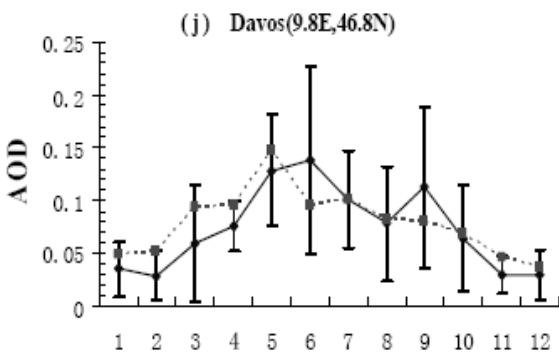
(h) La_laguna(16.3W,28.5N)



(i) Venice(12.5E,45.3N)



Comparisons of simulated total AOD (dashed line) with those measured (solid line) at 18 AERONET sites at 550 nm. The error bar indicates the standard deviation of observed optical depth.



Comparisons of simulated total AOD (dashed line) with those measured (solid line) at 18 AERONET sites at 550 nm. The error bar indicates the standard deviation of observed optical depth.

Comparison simulated AOD with CARSNET

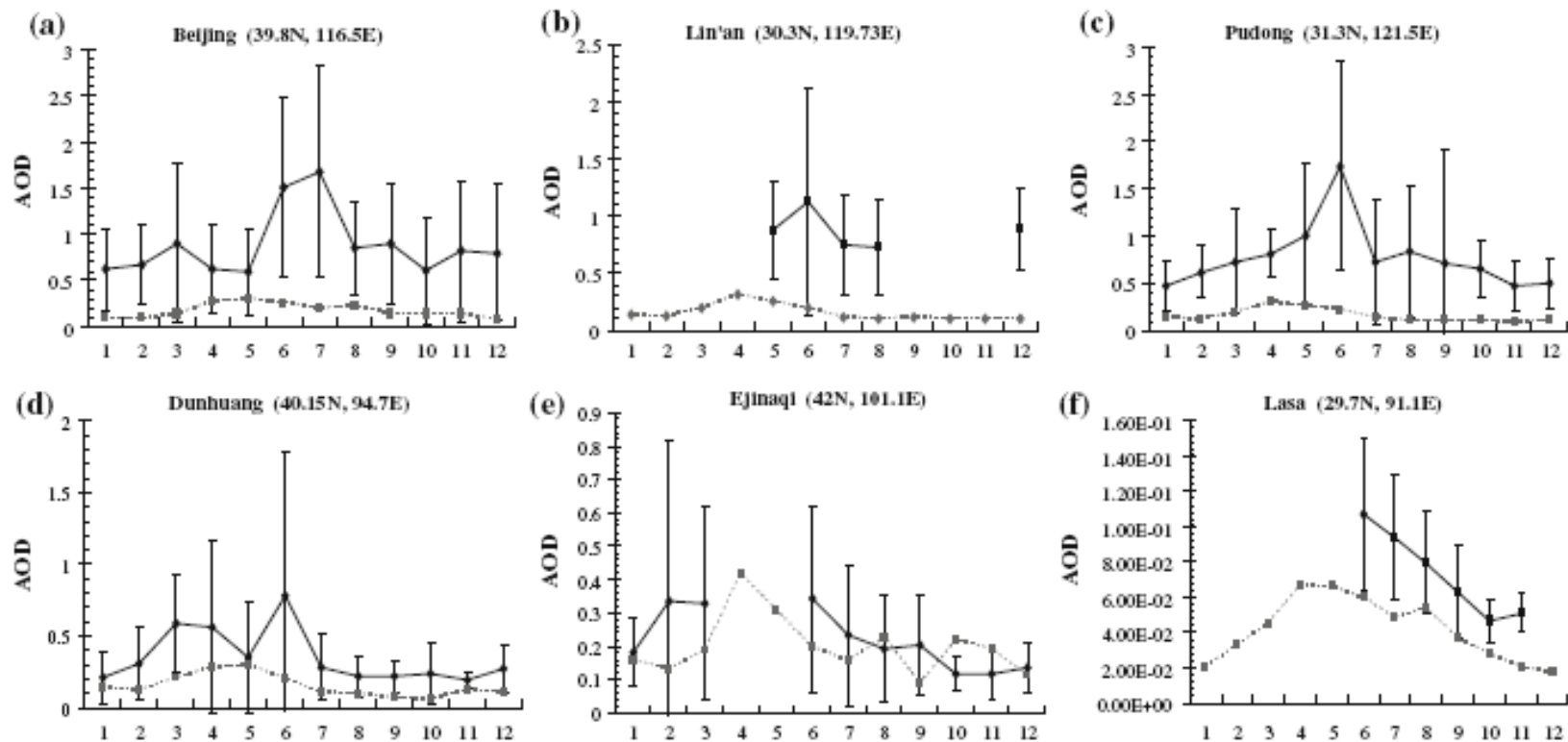
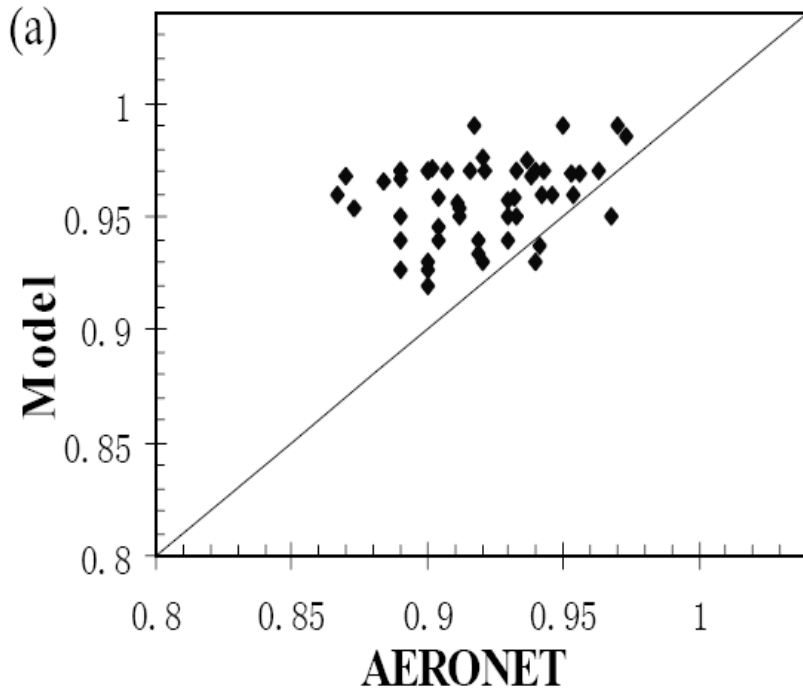


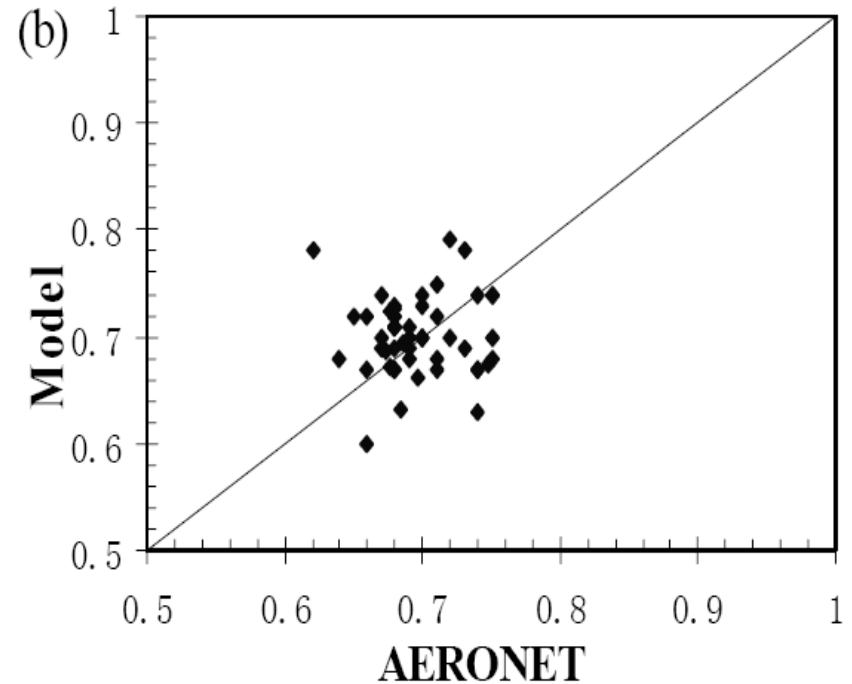
Fig. 4 Comparisons of simulated total AOD (*dashed line*) with those measured (*solid line*) at 6 CARSNET sites at 550 nm. The *error bar* indicates the standard deviation of observed optical depth. The

CARSNET data are from China Meteorological Administration Aerosol Remote Sensing NETWORK

Mean difference: 4%

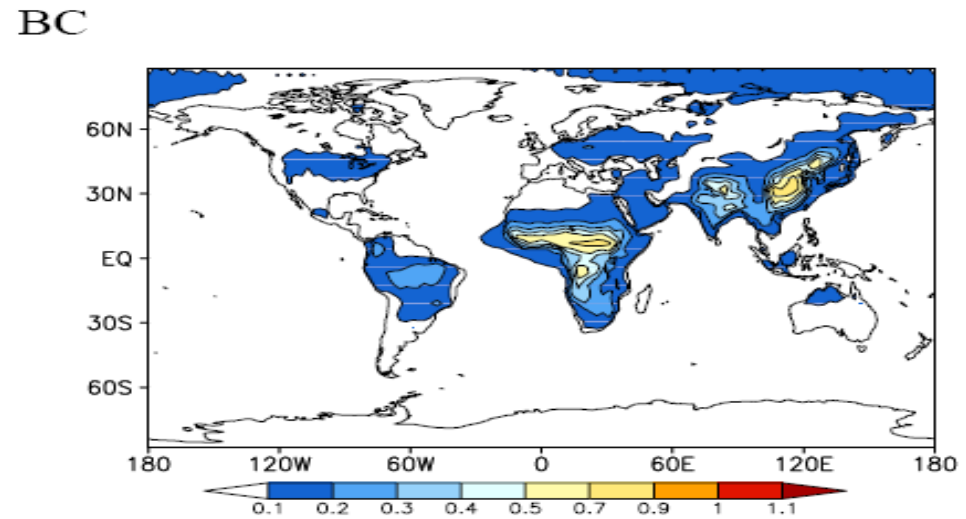
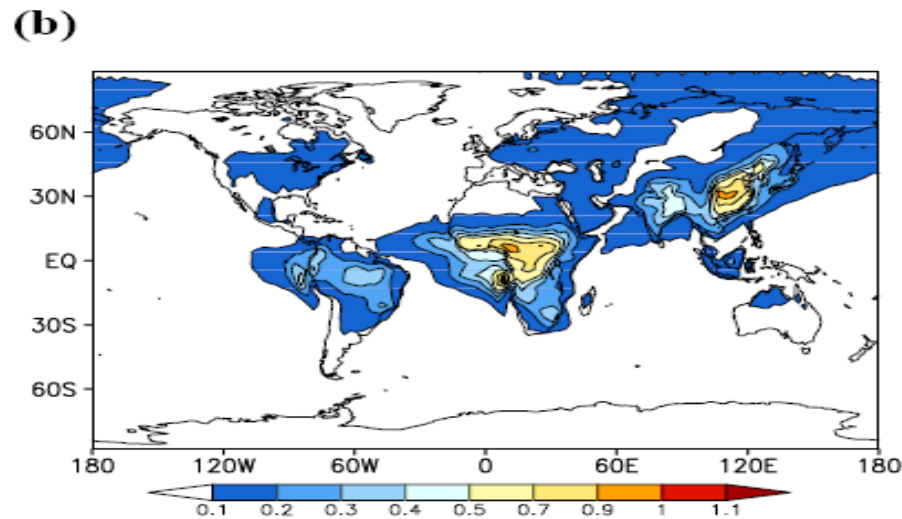
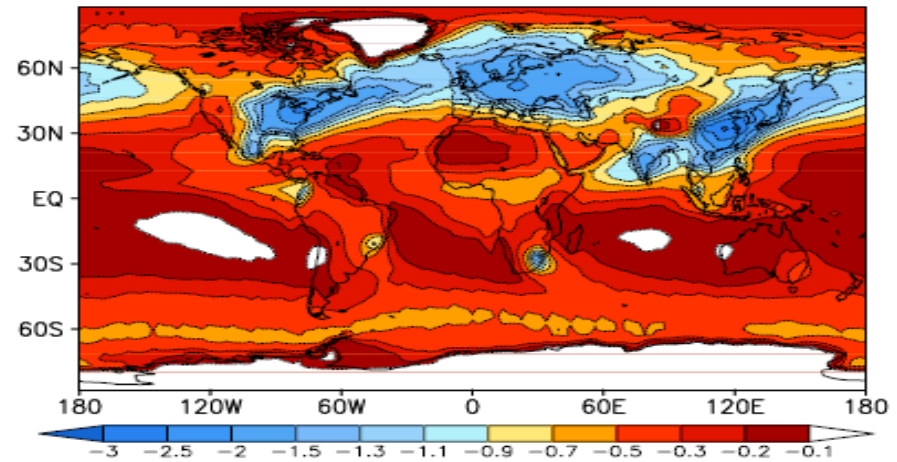
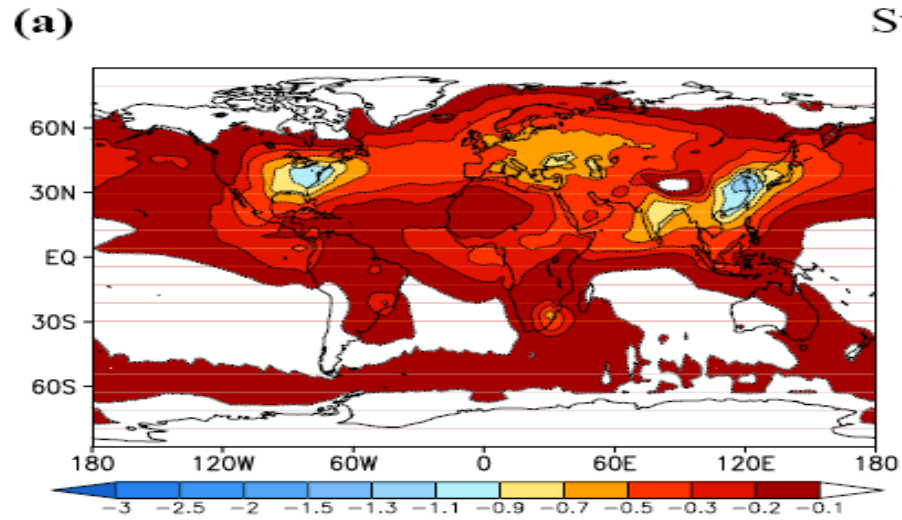


Mean difference: 5%



Scatterplots of the simulated (a) single scattering albedo and (b) asymmetry parameter vs AERONET at 52 sites at 550 nm

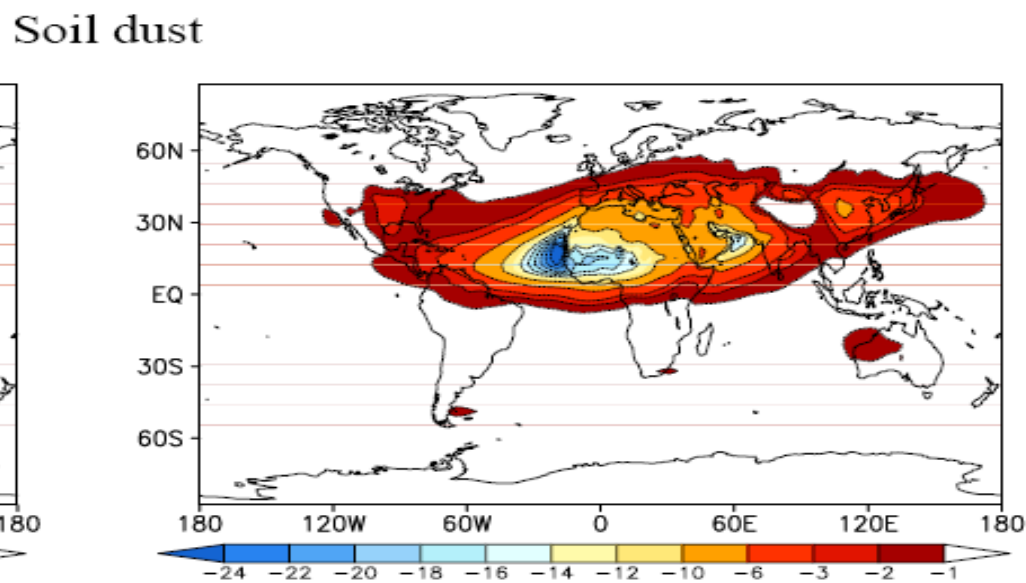
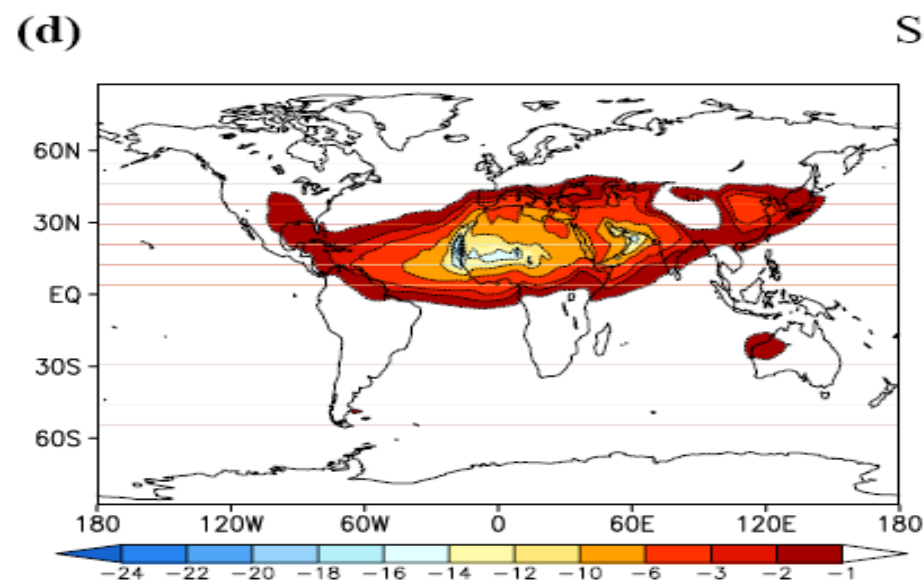
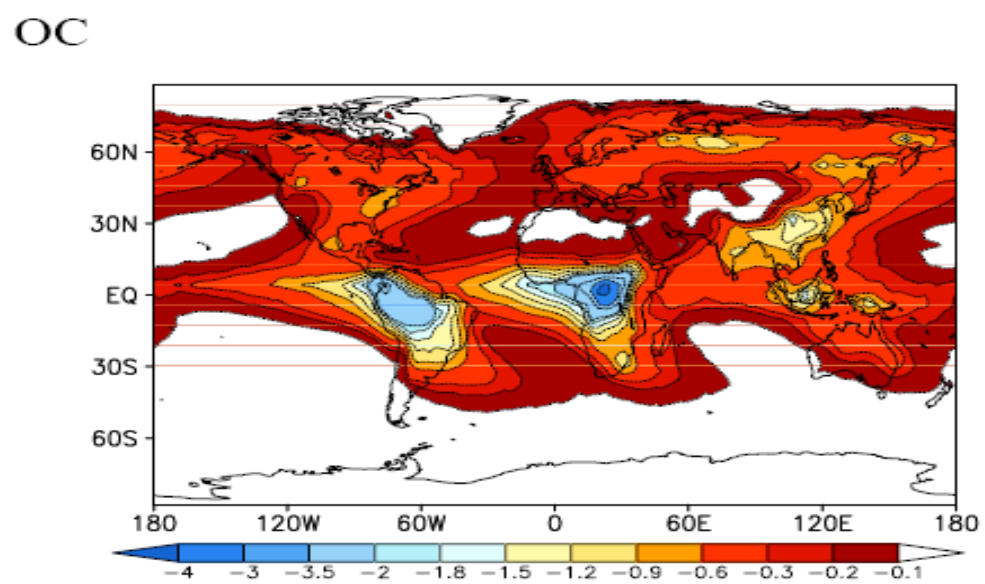
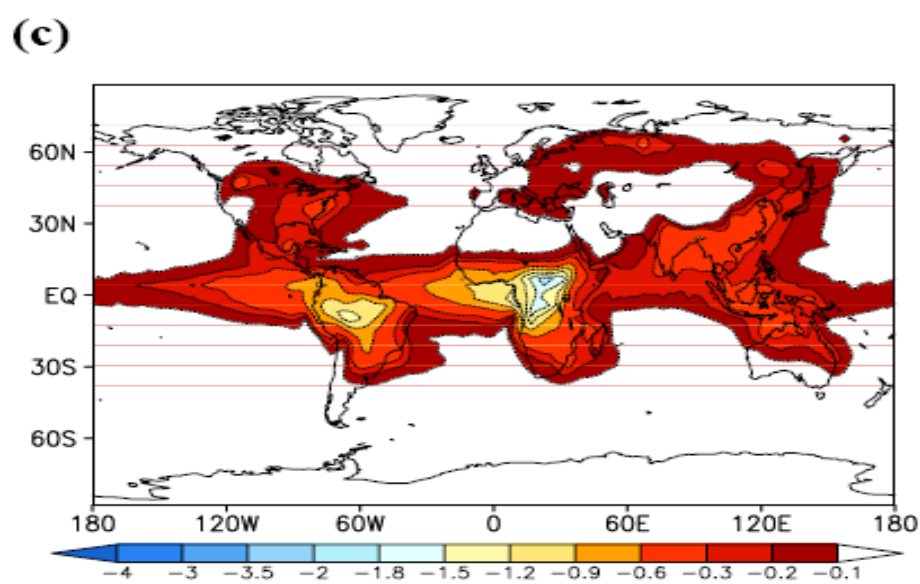
Direct radiative forcing (DRF) due to aerosols



All-sky

Clear-sky

Annual mean distributions of the simulated DRFs (W m^{-2}) due to aerosols at the TOA under all-sky (left) and clear-sky (right) conditions

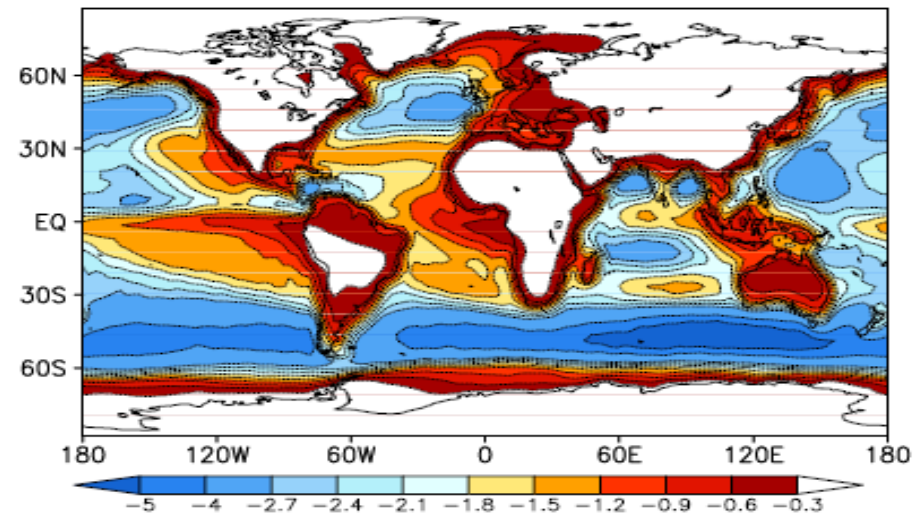
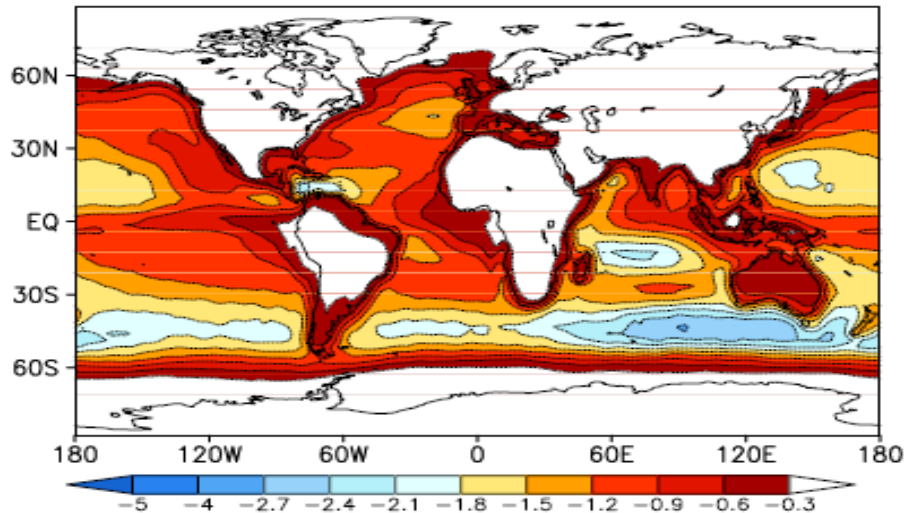


All-sky

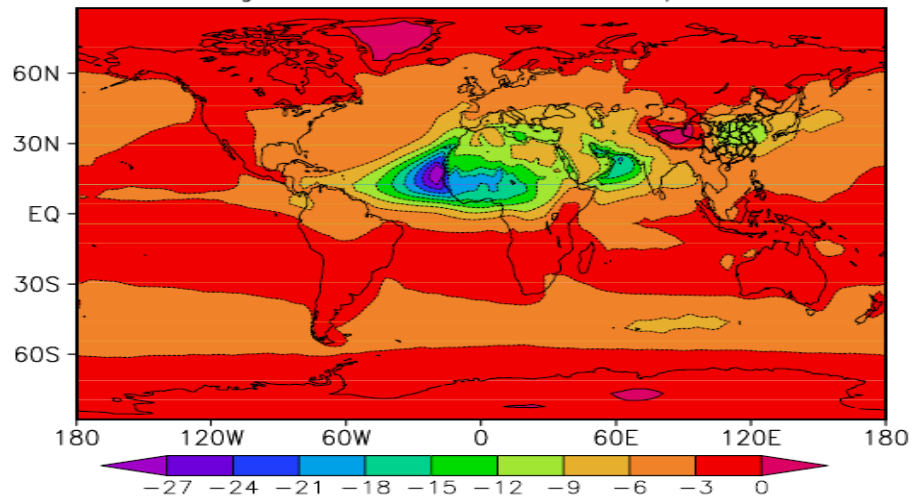
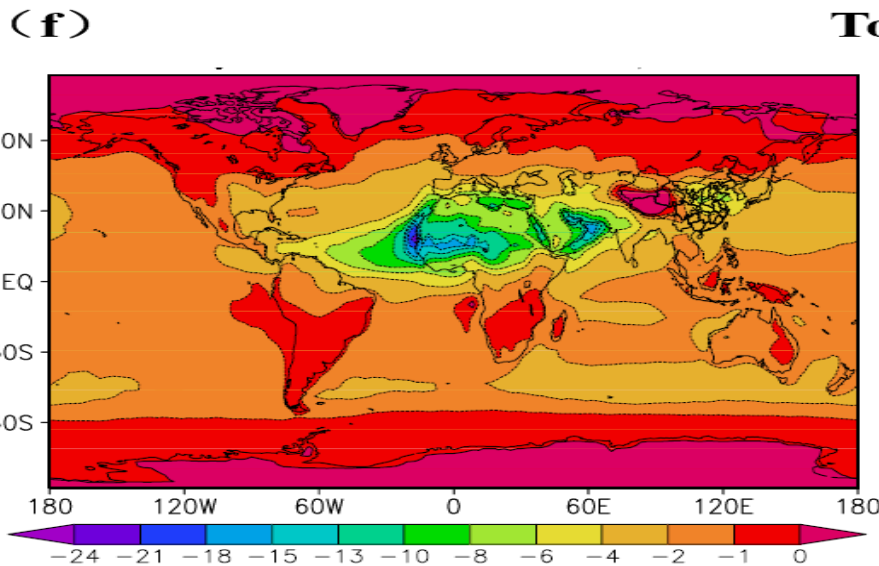
Clear-sky

Annual mean distributions of the simulated DRF (W m^{-2}) due to aerosols at the TOA under all-sky (left) and clear-sky (right) conditions

Sea salt



Total



All-sky

Clear-sky

Annual mean distributions of the simulated DRF ($W m^{-2}$) due to aerosols at the TOA under all-sky (left) and clear-sky (right) conditions

Simulated annual hemispherical and global mean DRF due to different aerosol components at the TOA and surface under all-sky and clear-sky conditions ($W m^{-2}$)

	All sky			Clear sky		
	NH	SH	Global	NH	SH	Global
Sulfate	-0.28(-0.3)	-0.1(-0.11)	-0.19(-0.21)	-0.68(-0.71)	-0.26(-0.27)	-0.47(-0.49)
BC	+0.12(-0.24)	+0.06(-0.15)	+0.1(-0.19)	+0.09(-0.32)	+0.03(-0.18)	+0.06(-0.25)
OC	-0.16(-0.27)	-0.13(-0.21)	-0.15(-0.24)	-0.39(-0.52)	-0.27(-0.36)	-0.33(-0.44)
Dust	-1.7(-3.8)	-0.13(-0.21)	-0.9(-1.98)	-2.6(-4.8)	-0.2(-0.29)	-1.42(-2.55)
Sea salt	-0.61(-0.71)	-1.0(-1.2)	-0.83(-0.94)	-1.1(-1.3)	-2.0(-2.2)	-1.54(-1.72)
Anthropogenic aerosols			-0.23(-0.59)			-0.73(-1.13)
All aerosols			-2.03(-3.63)			-3.84(-5.61)

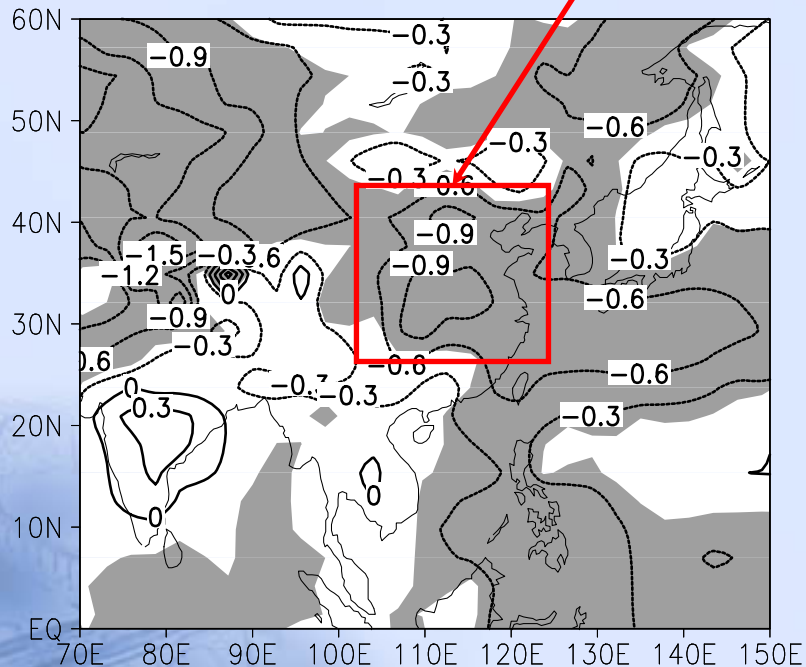
**Notes: the values in parentheses represent the corresponding surface forcing.
NH = Northern Hemisphere, SH = Southern Hemisphere**



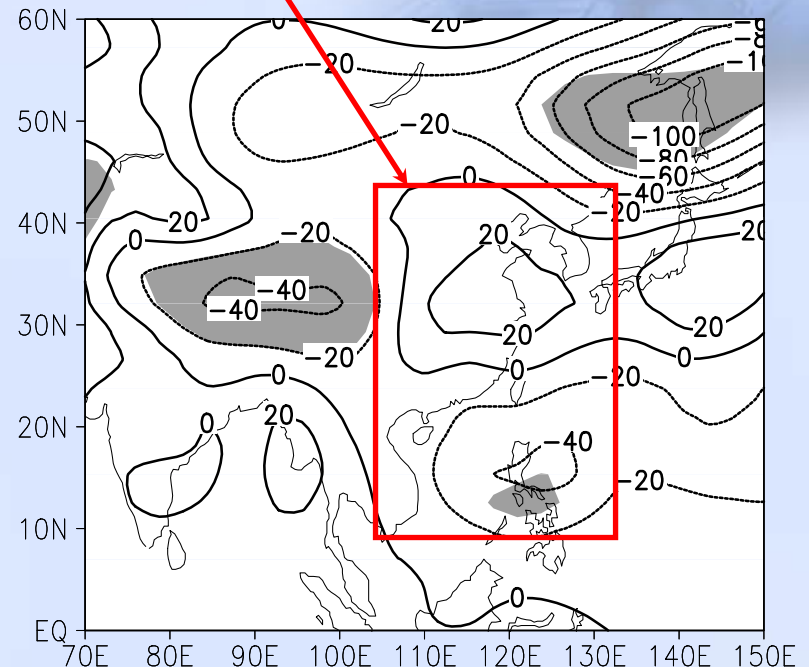
**The effects of sulfate, BC and OC aerosols
on the East Asian summer monsoon**

□ The results obtained in this work showed that the summer average DRFs due to Sulfate, BC, and OC in East Asia ($20^{\circ}\sim 40^{\circ}\text{N}$, $100^{\circ}\sim 140^{\circ}\text{E}$) at the TOA and surface were **-1.4 W m^{-2}** and **-3.3 W m^{-2}** , respectively, leading to decreases of the summer means of **0.58°C** surface temperature and **0.14 mm d^{-1}** precipitation rate in this area, respectively.

The differences of land-sea surface temperature and surface pressure were reduced in East Asian monsoon region due to these aerosols.

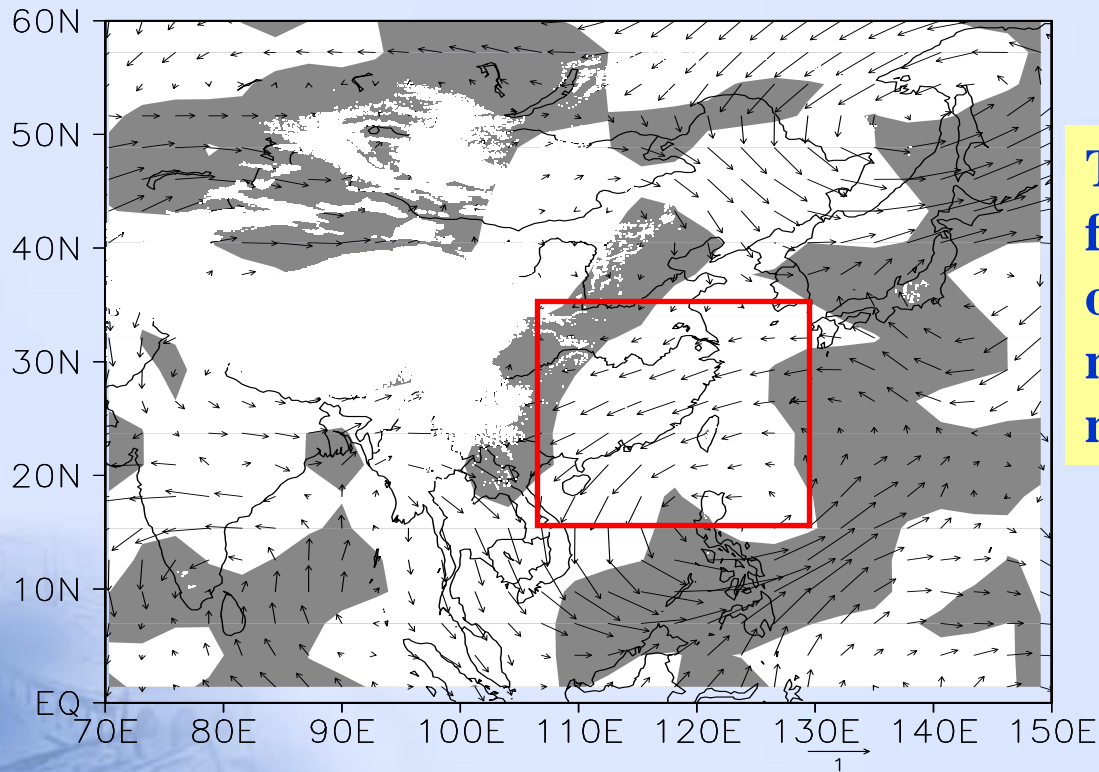


(a)



(b)

The changes of JJA mean (a) surface temperature (°C) and (b) surface pressure (Pa) due to the sulfate, BC and OC aerosols. The shade indicates a confidence level of 90% from the *T*-test



The enhanced northeasterly flow weakened the intensity of the southwest summer monsoon and suppressed the monsoon precipitation.

The changes of JJA mean wind field at 850 hPa (vector) due to sulfate, BC and OC aerosols. The shade shows the differences of moisture flux divergence due to aerosols are negative integrated from 850 to 700 hPa

Publications

- 1. Zhang, H., Z. L. Wang, Z. Z. Wang, and Coauthors, Simulation of direct radiative forcing of aerosols and their effects on climate using an interactive AGCM-aerosol coupled system, *Climate Dynamics*, 2011, online, published.**
- 2. Zhang, H., Z. L. Wang, P. W. Guo, Z. Z. Wang, A modeling study of the effects of direct radiative forcing due to carbonaceous aerosol on the climate in East Asia. *Adv. Atmos. Sci.*, 2009, 26(1), 1-10.**
- 3. Wang, Z. L., H. Zhang, X. S. Shen, S. L. Gong, and X. Y. Zhang, Modeling study of aerosol indirect effects on global climate with an AGCM. *Adv. Atmos. Sci.*, 2010, 27(5), 1064-1077, doi: 10.1007/s00376-010-9120-5.**
- 4. Wang, Z. L., H. Zhang, P. W. Guo, The effects on Asian summer monsoon due to black carbon aerosol in the South Asia. *Plateau Meteorology (in Chinese)*, 2009, 28(2), 419-424.**
- 5. Wang, Z. L., P. W. Guo, and H. Zhang, A numerical study of direct radiative forcing due to black carbon and its effects on summer precipitation in China. *Climatic and Environmental Research (in Chinese)*, 2009, 14(2), 161-171.**

The background features a faint, light blue illustration of a hand holding a scroll, which is centered behind the text. The entire scene is framed by a decorative border of small, dark blue rectangular tiles at the top and bottom edges.

Thank you!